NASA TECHNICAL MEMORANDUM

NASA TM X- 71499

NASA TM X- 71499

ACOUSTIC CHARACTERISTICS OF EXTERNALLY BLOWN FLAP SYSTEMS WITH MIXER NOZZLES

by Jack H. Goodykoontz, Robert G. Dorsch, and Jack M. Wagner
Lewis Research Center
Cleveland, Ohio 44135

TECHNICAL PAPER proposed for presentation at
Twelfth Aerospace Sciences Meeting sponsored by
the American Institute of Aeronautics and Astronautics
Washington, D.C., January 30 - February 1, 1974

ACOUSTIC CHARACTERISTICS OF EXTERNALLY BLOWN FLAP SYSTEMS WITH MIXER NOZZLES

by Jack H. Goodykoontz, Robert G. Dorsch, and Jack M. Wagner

Lewis Research Center

ABSTRACT

Noise tests were conducted on a large-scale cold-flow model of an engine-under-the-wing externally blown flap lift augmentation system employing a mixer nozzle. The mixer nozzle was used to reduce the flap impingement velocity and, consequently, try to attenuate the additional noise caused by the interaction between the jet exhaust and the wing flap. Results from the mixer nozzle tests are summarized and compared with the results for a conical nozzle. The comparison showed that with the mixer nozzle, less noise was generated when the trailing flap was in a typical landing setting (e.g., 60°). However, for a takeoff flap setting (20°), there was little or no difference in the acoustic characteristics when either the mixer or conical nozzle was used.

Comparisons are also made between the flap noise results from the cold-flow facility and full-scale mixer-nozzle engine tests. A simplified method of scaling based on the flow capture area at the flap impingement point is used to scale the sound pressure level data from the two separate tests to compensate for the difference in physical size of the models. Frequency shift was accounted for by the ratio of the total equivalent diameters of the two nozzles.

The results show good agreement between the spectra for the cold-flow, large-scale model and the engine tests. Overall sound pressure levels below the wing were proportional to the sixth power of the peak flap impingement velocity.

INTRODUCTION

With the advent of commercial short-haul STOL aircraft, the noise conditions imposed upon the community will become more severe because of the nearness of the airport to densely populated areas and

also because of the additional noise created by the STOL aircraft design requirements. One of the design requirements is lift augmentation. The engine-under-the-wing externally blown flap (EBF) system is one method to increase the lift capability of STOL aircraft during takeoff or landing. Lift augmentation is obtained by lowering the flaps directly into the engine exhaust. However, the impingement of the high velocity airstream on the flap surfaces causes a substantial increase in the noise level of the aircraft. The flap interaction noise appears to be proportional to the surface area of the flaps scrubbed by the jet exhaust and to the sixth power of the jet impingement velocity (ref. 1). Reducing the impingement velocity (while maintaining acceptable lift characteristics) appears to offer promise of reduction in flap interaction noise.

The impingement velocity can be reduced by employing a mixer nozzle at the engine exhaust to cause rapid decay of the exhaust jet velocity (ref. 2). A mixer nozzle is a multi-element nozzle consisting of an array of small flow passages instead of a single large flow passage with the same total area. The velocity of the individual small jets making up the exhaust decreases rapidly by mixing with the surrounding air prior to reaching the flap station.

Various types of mixer nozzles have been tested in an effort to reduce engine exhaust-jet noise (ref. 3). However, the concept of using a mixer nozzle to suppress flap noise in an EBF system is relatively new. Consequently, there is presently insufficient experimental evidence for determining the merit, or lack of merit, of such a system. Related NASA work in this general area is reported in references 4 to 6, where data were obtained using a full size turbofan engine. Concurrently, noise tests were conducted at the Lewis Research Center by using small (nozzle equivalent diameter = 2 3/8 inches) and large (15 3/4 inches) scale EBF models, and by simulating engine exhaust flow with cold (45 to 80° F) pressurized air. The detailed results of these tests are given in references 7 to 9.

This paper shows the effectiveness of a particular type of mixer (or decayer) nozzle in reducing flap noise in an EBF lift augmentation system. The effectiveness is judged by comparing experimental noise data obtained when the mixer nozzle is employed with that from an EBF system using a conical nozzle with the same flow area. Seven-lobe mixer nozzle data from a large-scale cold-flow facility using a two-flap wing system (ref. 8) are compared with conical nozzle data taken in the same facility and with the same wing-flap system (ref. 10). The total equivalent diameter of the mixer nozzle was 15 3/4 inches. The wing model used in the cold-flow tests had a span of 108 inches and a chord length of 82 inches.

In addition, a comparison is shown for the cold-flow mixer nozzle EBF results and those from the full-size turbofan engine EBF test of reference 6. For the engine tests, a 12 lobe mixer nozzle (co-planar-decayer) was used, having a total equivalent diameter of 37.6 inches. Span length of the wing was 76 inches and chord length, 153 inches.

APPARATUS AND PROCEDURE

Cold-Flow Facility

Airflow system.- The airflow system is shown schematically in figure 1. Dry cold air (45 to 80°) was supplied to a 16-inch diameter gate shutoff valve through an underground pipeline from the Center's air supply system (150 psig max). Air flow rate and nozzle pressure ratio (nozzle total pressure divided by ambient atmospheric pressure) were set by adjustment of a 10-inch diameter butterfly flow control valve.

A muffler system installed in the line downstream of the flow control valve attenuated internal noise caused primarily by the flow control valve. Essentially, the muffler system consisted of perforated plates and dissipative type mufflers. The perforated plates were located immediately downstream of the flow control valve (40 percent open area) and at the entrances and exit of the first dissipative muffler (20 percent open area). Both mufflers were sections of pipe that housed crossed splitter plates oriented at right angles to one another so that the flow was divided into four channels. All internal surfaces of the muffler pipes and surfaces of the splitter plates were covered with acoustic absorbent material. The second muffler was located downstream of the last 45° elbow in the air flow line to take advantage of the reflections caused by turning the flow. In addition, the flow system was wrapped externally with fiberglass and leaded vinyl sheet to impede direct radiation of internal noise through the pipe wall.

Two screens were placed in the air line downstream of the last muffler to improve the flow distribution to the nozzle. Total pressure and temperature were measured directly upstream of the nozzle. Nozzle exhaust velocities were calculated from the isentropic gas dynamic equations.

Model description.- A photograph of the experimental set-up is shown in figure 2. The wing section had a span length of nine feet and was mounted with the spanwise direction vertical. The nozzle axis was 12 3/4 feet above grade and five feet above the wing mounting

platform. Dimensions and details of the configuration are shown in figure 3. The wing section (fig. 3(a)) had two flaps that could be placed in any one of three positions: (1) retracted; (2) leading flap 10° with respect to the wing chord line; trailing flap 20°; and (3) leading flap 30°, trailing flap 60°. Length of the chord line with the flaps retracted was 82 inches. The wing was mounted with a 5° angle of attack between the wing chord line and nozzle axis. With the trailing flap lowered to the 60° setting the nozzle axis intersected the flap at its 20 percent chord position. With a 20° trailing flap setting the nozzle axis was below the flap. The distance from the mixer nozzle exit to the 60° trailing flap, measured along the nozzle axis, was 72 inches. Location of the conical nozzle (ref. 10) relative to the wing is also shown in the figure. The conical and mixer nozzle axes were the same distance below the wing.

In figure 3(b) the dimensions of the mixer nozzle and its orientation relative to the wing are given. The nozzle was designed to reduce the exhaust gas velocity at the flap station (72 inches downstream of nozzle exit) to approximately 60 percent of the nozzle exhaust velocity. Alternate lobes were canted 10° outward from the nozzle axis to improve the velocity decay characteristics of the nozzle (ref. 2). The nozzle was originally tested as an eight-lobe nozzle with a straight lobe placed nearest the wing. Results showed, however, that the seven-lobe arrangement in figure 3(b) was quieter as a result of reducing the scrubbing action of the flow on the underside of the wing. Exit area for the seven-lobe nozzle was 194.5 square inches which is equivalent to the area of a circular nozzle with a diameter of 15 3/4 inches. Equivalent diameter for a single lobe was 5.95 inches. Nozzle coefficient (ratio of measured to ideal flow rate) was close to unity. External aerodynamic characteristics were not considered in the design of the nozzle since they were assumed to be of little importance in the static tests described herein.

Test procedure.- Far field noise data were taken over a range of nozzle pressure ratios for the various trailing flap settings. Pressure ratios (nozzle total pressure divided by atmospheric pressure) ranged from 1.2 to 1.7, and nozzle total temperatures from 46 to 77° F, giving a range in calculated nozzle exhaust velocities from 550 to 950 feet per second.

Velocity profiles in the exhaust jet on the centerline of two diametrically opposed lobes were calculated from total pressure measurements made at various locations downstream of the nozzle exit. It was assumed that the total temperature in the exhaust jet was the same as that measured upstream of the nozzle exit and that the static pressure was the same as atmospheric pressure.

Acoustic instrumentation and analysis.- Noise measurements were made with twenty 1/2 inch condenser microphones placed on a 50-foot-

radius circle centered three feet downstream of the nozzle exit. The microphone circle was in a horizontal plane through the nozzle axis 12 3/4 feet above a hard paved surface.

The noise data were analyzed by a 1/3 octave band spectrum analyzer which determined sound pressure level spectra referenced to 0.0002 microbar. Three samples of data were taken at each microphone, averaged, and corrected for atmospheric attenuation to give lossless sound pressure level data at 50 feet. All data in this report are lossless unless stated otherwise. Overall sound pressure levels were calculated from the lossless SPL data. The data presented herein do not include ground reflection corrections.

Full Scale Engine Facility

Engine flap noise data were obtained during the study reported in reference 6 where an acoustically suppressed high-bypass turbofan engine was used with a co-planar-decayer nozzle and a section of a wing-flap system.

Orientation and dimensions of the nozzle and wing setup used in the full scale engine tests of reference 6 are shown in figure 4. The decayer nozzle from the engine tests (co-planar-decayer) had twelve lobes with a core exit area of 295 square inches and a fan exit area of 815 square inches. Fan and core flows exited in a common plane. Equivalent diameter of the nozzle based on the total exit area was 37.6 inches. As pointed out in reference 6, the decayer nozzle velocity profile at the nozzle exit showed that the peak core exhaust velocity was about 150 feet per second greater than the peak fan exhaust velocity at rated power. At lower power settings the core and fan exhaust velocities were about equal.

The wing segment was tapered in the spanwise direction and had a chord length of 154 inches at the engine centerline with the flaps retracted. The wing had three flaps that could be placed at various angular positions relative to the wing chord line.

Full scale engine data were taken for the three different axial distances from the nozzle exit to flap impingement point indicated in figure 4. Acoustic data taken with a trailing flap setting of 55° will be used for comparison with the cold-flow results reported herein since data from other settings common to both facilities were not available. Comparisons will be made for conditions and configurations that are approximately the same as the cold-flow tests. That is, tests with similar nozzle exhaust velocities, exhaust gas velocity decay rates, and spacing of the nozzle relative to the wing and flaps.

AERODYNAMIC RESULTS

In this section the aerodynamic characteristics of the cold-flow model will be discussed and then compared with data from the turbofan engine test.

Cold-Flow Model

Exhaust jet flow characteristics.- External flow characteristics downstream of the mixer nozzle and a conical nozzle are shown in figure 5 (wing removed). The axial distances given on the figure are the same as those from the nozzle exits to the 60° flap, measured along the nozzle axes, when the wing is in place. The results for the conical nozzle were obtained during the study reported in reference 10 and are included to illustrate the differences in the flow field for the two nozzle configurations. The conical nozzle had a throat diameter of 13 inches compared to the equivalent diameter of 15 3/4 inches for the mixer nozzle. However, calculation of peak velocity for a 15 3/4 inch conical nozzle at 94 inches downstream of the nozzle exit (ref. 2) gave a value of 913 feet per second, compared to 905 feet per second measured for the 13 inch nozzle. In addition, the profile width for a 15 3/4 inch conical nozzle (at X = 94 inches) was about 40 inches, compared to 39 inches for the 13 inch nozzle. Therefore, the results presented for the 13 inch nozzle can be considered to be a close approximation to those which would be obtained using an exact size nozzle.

In figure 5(a), the radial distribution of velocity is given for the mixer and conical nozzles. The velocity profiles across the mixer nozzle are characterized by velocity peaks displaced radially from the nozzle axis indicating that the flow is still in the development stage. Complete coalescence of the flow occurs farther downstream and a typical single parabolic shape profile is formed (ref. 7). The profile across the straight lobes is not symmetrical about the axis due to the asymmetry of the seven-lobe nozzle. The peak velocity from the straight lobe (at X = 72 inches) is about 67 percent of the nozzle exhaust velocity. Only a small amount of jet scrubbing on the underside of the fixed portion of the wing occurs (when the wing is in place) as a result of the small jet spreading half-angle (approximately 4°), and the orientation of the nozzle lobes relative to the wing (fig. 3(b)).

The width of the flow field across the canted lobes is approximately 75 percent greater than that across the straight lobes (fig. 5(a)). Two velocity peaks are observed. The outer peak represents flow directly from the canted lobe, whereas the smaller inner peak indicates ventilation velocities induced by flow from the straight

lobe. Peak velocity from the canted lobe is about 10 percent less than that from the straight lobe as a result of better mixing with ambient air and/or less interference from surrounding jets of the nozzle.

Results from the conical nozzle tests in figure 5(a) show that the peak velocity (at X = 94 inches) is 95 percent of the nozzle exhaust velocity. This small reduction in velocity implies that the conical nozzle-wing combination should have noise levels that are considerably greater than when the mixer nozzle is used. However, the flap impingement area is also an important parameter in determining the level of the jet exhaust flap interaction noise. An indication of the impingement area can be shown by examining the flow-field envelope at the flap impingement station.

Flow-field envelopes for the mixer and conical nozzles are shown in figure 5(b). The axial location of the envelopes is shown in the inset of the figure (at the trailing flap impingement station). Projected flap area, (area perpendicular to nozzle axis), is superimposed on the envelopes. Zero velocity loci were constructed using the data of figure 5(a). The locus for the conical nozzle was assumed to be circular. It was necessary to estimate the shape of the locus for the mixer nozzle as a result of its complex flow field. This approach is obviously an over-simplification of the real process but gives an insight into the problem of determining the impingement area. Location of peak velocities for the two nozzles are indicated by the symbols. With the mixer nozzle, the flaps are subjected to six areas of relatively high velocity (area sizes are arbitrary at this time). The inner minor peak velocity from the canted lobe is omitted (fig. 5(a)). When the conical nozzle is used, high velocity flow strikes the flaps in a single area. Essentially, the mixer nozzle causes impingement over a greater flap area than the conical nozzle but at a lower velocity. The net effect on the jet-flap interaction noise is discussed in subsequent sections.

Velocity decay data, with the wing removed, are summarized in figure 6. In figure 6(a) the peak jet velocity downstream of the nozzle exit for a 13-inch-diameter conical nozzle (ref. 10) is compared with the mixer nozzle used herein. Straight-lobe peak velocities are given in the figure for the mixer nozzle. The rate of decay for the mixer nozzle is much greater than that for the conical nozzle. At a distance of 72 inches, for example, the peak jet velocity using the mixer nozzle is approximately 2/3 of the exhaust velocity, whereas for the conical nozzle, the reduction is negligible.

In figure 6(b)), the velocity data are presented in terms of an axial distance parameter developed from an experimental program at Lewis (ref. 2). In reference 2, the parameter is based on the equivalent diameter of a single flow element, whereas in figure 6(b) the

total equivalent diameter of the nozzle is used instead. The figure is presented to show, in a qualitative way, the effect of increasing the number of flow passages (or lobes) of a nozzle. The solid curve in the figure is calculated for a typical single conical nozzle using the equations given in reference 2. Data points from the 13-inch-conical nozzle used herein for comparison purposes agree adequately with the prediction curve.

The dashed curves are estimates made for nozzles with different numbers of lobes. Data from the seven-lobe mixer nozzle are in general agreement with the estimated prediction. The curve representing the coalescing core region (A-A in fig. 6(b)) is based on small scale model studies of reference 2. In the figure, the results show that by increasing the number of lobes, for a given total nozzle area and nozzle exhaust velocity, the shorter the distance for a given velocity decay. However, by increasing the number of lobes while keeping the same nozzle exhaust exit area means that the overall dimension of the nozzle must increase. In addition, for a given lobe spacing, the core starts coalescing at a position closer to the nozzle exit with a low rate of velocity decay thereafter.

Comparison with Full Size Engine Data

In figure 7 the exhaust jet velocity profiles are given for the seven-lobe cold-flow and 12-lobe full-size engine nozzles (wings removed). The radial distance is normalized to account for differences in the size of the models. The profiles for the cold-flow nozzle is at an axial distance downstream of the nozzle exit which is the same as that from the nozzle exit to the impingement point on the trailing flap when the wing is in place. The axial location of the profile for the 12-lobe nozzle (100 inches) is close to the trailing flap impingement point for that test (91 inches). The profile shape for the straight lobe of the cold-flow nozzle is similar to that of the engine nozzle with the peak velocities occurring at approximately the same relative distance from the nozzle axis. However, the peak velocity from the canted lobe occurs at a greater relative distance and is about 10 percent lower than the straight lobe peak velocity.

The velocity decay characteristics of the two nozzles are shown in figure 8 in terms of the ratio of peak exhaust jet velocity to nozzle exhaust velocity as a function of the distance downstream of the nozzle exit. The peak velocity from the straight lobes is used for the seven-lobe nozzle. Both nozzles have a high rate of velocity decay. At the flap impingement point the seven and 12-lobe nozzles reduce the peak jet velocity to 62 and 53 percent, respectively, of the nozzle exhaust velocity.

ACOUSTIC RESULTS

This section presents the acoustic results of the mixer nozzle - EBF system. First, the cold-flow data are discussed. Data are given to show how the acoustic characteristics of the mixer nozzle alone differ from those of a conical nozzle with the same exhaust flow area. Flap noise is then summarized for the mixer nozzle followed by a comparison of the results with a conical nozzle. Finally, the mixer nozzle flap noise results of the cold-flow tests are compared to full scale engine test results.

Cold-Flow Model

Nozzle alone.- Noise data for the mixer nozzle alone are compared to the results obtained from a conical nozzle alone in figure 9. Data for a 13-inch-diameter conical nozzle were obtained as part of the test program reported in reference 10. The data from the conical nozzle were scaled to the mixer nozzle size (D_{et} = 15.75 inches) by application of the scaling laws described in reference 10. Measured sound pressure levels of the conical nozzle were increased by 1.7 dB as a result of the difference in nozzle exhaust area. The frequency was lowered by one 1/3 octave band by assuming that the spectra could be scaled by using the Strouhal relation between frequency and diameter. Total equivalent diameters were used for this relation. In figure 9(a) the overall sound pressure level (OASPL) directivity pattern for the two nozzles is shown. The patterns are similar in shape except for the location of the peak OASPL, with the conical nozzle peak level occurring closer to the jet exhaust. Overall sound pressure levels with the mixer nozzle are comparable to those with the conical nozzle.

Sound pressure level (SPL) spectra at 85° are compared in figure 9(b). The mixer nozzle has lower levels of low frequency noise, but higher levels of noise in the high frequency range. In figure 9(c) the spectra at a location near the jet exhaust (145° from the nozzle inlet), which is near the location where the peak OASPL occurs, are shown. Both nozzles have a higher level in low frequency noise content than that measured at 85° from the nozzle inlet (fig. 9(b)). The general trends, however, are the same in that the mixer nozzle is quieter in the low frequency range and louder in the high frequency range. Increase in high frequency noise with the mixer nozzle is caused by the small dimensions of the individual flow passages.

Flap noise.- In this section the data from the mixer nozzle-wing combination are presented and summarized, followed by a comparison of the results obtained using the mixer and conical nozzles.

The variation in the flap noise radiation field is shown in figure 10 for various trailing flap settings. An angle of 85° from the nozzle inlet represents a location directly under the wing (perpendicular to wing chord line) since the wing is canted 5° with respect to the nozzle axis (fig. 3(a)). The directivity curves of figure 10(a) show that an increase in OASPL occurs below the wing (0 to 135°) when the flaps are lowered into the jet exhaust in addition to a redirection (or rotation) of the noise field. The peak OASPL for a trailing flap setting of 60° occurs at 70° from the nozzle inlet whereas for the retracted and 20° flap settings it occurs at approximately 125°. From zero to 130° the noise levels with retracted flaps are higher than those for the nozzle alone indicating reflection of the nozzle noise by the wing and possibly a small amount of scrubbing noise.

The SPL spectra at 85° from the nozzle inlet are shown in figure 10(b). As indicated in the figure, lowering the flaps into the jet exhaust causes, primarily, an increase in the low frequency noise of the system.

Overall sound pressure level as a function of nozzle exhaust velocity for the various trailing flap settings, as well as for the nozzle alone, is shown in figure 11. Figure 11(a) shows the variation at a location directly below the wing (85°). The slope of the curves with the wing in place (7th power) is less than that for the nozzle alone (8th power). In addition, the difference in OASPL for the 60° and 20° flap setting is only 1 to 1.5 dB for a given velocity at this position under the wing.

In figure 11(b) the radial peak OASPL is plotted as a function of nozzle exhaust velocity. Note that the peak OASPL occurs at different angles from the engine inlet for the different configurations (shown in fig. 10(a)). Again, with the 60° and 20° flap setting, the variation in OASPL is proportional to the 7th power of velocity. With the flaps retracted, and for the nozzle alone, an 8th power relation is followed.

Peak OASPL as a function of peak flap impingement velocity for the configurations with the flaps deflected (trailing flap at 20° and 60°) is shown in figure 12. Peak flap impingement velocities were estimated from the velocity decay data for the nozzle alone as presented in figure 5(a). Figure 12 shows that the peak OASPL varies as flap impingement velocity raised to the 6th power. The same relation with impingement velocity also exists for the variation in OASPL at 85° from the nozzle inlet.

Comparison with conical nozzle.- Comparison between the noise data for the mixer nozzle and a conical nozzle blowing on the wing-flap segment at the same nozzle exhaust velocity is shown in figure 13. In

figure 13(a) the OASPL directivity pattern is shown for the portion of the acoustic circle under the wing. With a trailing flap setting of 60° the mixer nozzle gives results that are 5 to 6 dB quieter than the conical nozzle. However, with a 20° flap setting the sound levels with either nozzle are approximately equal over a large portion of the acoustic circle. This result is attributed to the difference between the flow fields downstream of the exit plane of the nozzles. The peak free stream jet velocity from the conical nozzle occurs on the nozzle centerline. With the configuration used herein, when the trailing flap was raised from a 60° setting to 20°, the peak velocity from the conical nozzle did not impinge on the flap surface. However, the peak velocity from the mixer nozzle still hits the 20° trailing flap because of its radial displacement (fig. 5(a)). The reduction in sound level that occurs when the trailing flap is raised from 60° to 20°, when the mixer nozzle is used, is believed to be caused primarily by the reduction in impingement area.

The SPL spectra at 85° for the two nozzles with the wing are shown in figure 13(b) for a trailing flap setting of 60°. A decrease in low frequency and an increase in high frequency noise occurs when the mixer nozzle is used. With the trailing flap in the 20° setting, figure 13(c), the low frequency noise for the two nozzles is about the same but the noise in the high frequency range is again greater for the mixer nozzle.

Peak OASPL as a function of peak flap impingement velocity for the mixer and 15.75-inch-diameter conical nozzles, is shown in figure 14 for a 60° trailing flap setting. Included in the figure are data for a three-flap wing used with the seven-lobe mixer nozzle (ref. 9). For the three-flap tests, the nozzle to wing distance perpendicular to the nozzle axis was increased (10 inches) so that the exhaust flow would not scrub the underside of the fixed wing. In addition, the flap geometry was adjusted so that the trailing flap of both the two and three-flap configurations was subjected to the same flow field (radial velocity distribution). Results for the two and three-flap wings are similar, except for the angular location of the peak OASPL. Therefore, any scrubbing noise occurring on the fixed wing with the two-flap configuration contributes very little to the overall noise level of the system.

Figure 14 shows that at a given flap impingement velocity, the noise level from the mixer nozzle is about 3.5 dB greater than that of the conical nozzle. The difference in noise level is caused by the larger impingement area that occurs when the mixer nozzle is used (fig. 5(b)).

In order to bring the data of figure 14 together on a single curve, the OASPL of the conical nozzle would have to be increased by an amount that is dependent on the ratio of the impingement areas of the mixer and conical nozzles. The exact value of impingement area to choose is

uncertain as a result of the differences in flow fields for the two nozzles at the flap impingement location (fig. 5). Two simplified approaches were tried in order to determine the impingement area ratio. The first method uses the projected flap area based on total jet width; that is, the rectangular area at the flap impingement location, A_p, formed by the product of the total width of the velocity profile and the distance from the wing chord line to the trailing edge of the trailing flap (measured perpendicular to the nozzle axis).

The results of this scaling method are shown in figure 15(a) where the normalized peak overall sound pressure level (OASPL - 10 log A_p) is plotted as a function of peak flap impingement velocity. The width of the profile for the mixer nozzle was taken as that across the canted lobes (fig. 5(a)). The results for the conical nozzle were obtained by using the basic data from the 13-inch-conical-nozzle-wing tests of reference 10. Figure 15(a) shows that the data fall within $\pm$2 dB of the faired curve. Therefore, this method is at best an approximation and gives results that are comparable to those obtained by scaling nozzle exit areas (fig. 14).

The second method (ref. 11) uses the area of impingement determined from the width of the velocity profile curve where the velocity is reduced to, arbitrarily, 80 percent of the peak velocity. This width is used as the diameter of the high velocity impingement area. As shown in figure 5(b) the conical nozzle has one area of high velocity surrounding the peak impingement velocity whereas the mixer nozzle has six high velocity areas which impinge on the flaps. The cross section of the mixer nozzle velocity profile at the 80 percent peak velocity location of each high velocity area was assumed to be circular in order to calculate the impingement area, A_i, for that nozzle.

The results of this scaling method are shown in figure 15(b) where the normalized peak overall sound pressure level (OASPL - 10 log A_i) is plotted as a function of peak flap impingement velocity. The good agreement indicates, as pointed out in reference 11, that the impingement area, A_i, can be used to accurately correlate the data. Thus, detailed information is needed on velocity profile shapes as well as peak flap impingement velocities in order to correlate flap noise data from two different nozzle shapes and/or sizes.

Comparison with full size engine data.- In figure 16 data are presented from the engine tests of reference 6 for different axial distances between the nozzle exit and impingement point on the 55° trailing flap. The variation in OASPL at 70° from the engine inlet is plotted as a function of peak flap impingement velocity with the nozzle-to-flap axial distance as a parameter. At a given axial distance (X) the OASPL varies approximately as the 6th power of peak

flap-impingement velocity for X values of 91 and 111 inches. At 165 inches the 6th power relation does not fit as well. However, even for the 165 inch distance, the data are within 1.0 dB of the 6th power curve for the range of velocities covered.

The increase in noise level when the nozzle to flap distance is increased, at a given flap impingement velocity, is believed to be caused by an increase in the high velocity impingement area. Impingement area increases as a result of the coalescence of the flow from the individual lobes of the mixer nozzle as the axial distance increases. As an example, consider the velocity profiles across the straight lobes of the cold-flow mixer nozzle shown in figure 17 for two different axial locations. The peak velocities and overall width of the profiles are approximately the same for both locations. However, the profile width in the high velocity region (for example at 80 percent of peak velocity) at an axial distance of 96 inches is greater than that at 72 inches. Consequently, the high velocity impingement area is greater. Farther downstream, and at the same peak velocity, the profile width in the high velocity region increases even further. Eventually, of course, complete coalescence occurs and a profile without the radially displaced peak velocities is formed. In order to bring the three sets of engine data in figure 16 to a single curve, sound pressure levels would have to be adjusted for differences in impingement areas (at the same flap impingement velocities). Therefore, information about the shape of the exhaust profile at the flap impingement station is needed to completely define the impingement areas.

Noise data are now compared from the two experiments for a trailing flap setting of 60° for the cold flow facility, and 55° for the engine facility. An axial distance between nozzle and flap of 72 inches for the cold flow tests and 91 inches for the engine tests were used for the comparison since the radial velocity profiles at the flap impingement station had similar shapes (fig. 7) so that in scaling the data it was only necessary to account for the difference in the size of the models and the exhaust plumes. The projected flap area method was used to approximately scale the sound pressure levels since detailed velocity profile data were not available for the engine tests. It was also assumed that frequencies could be scaled by using the Strouhal relation between frequency and total equivalent diameters of the nozzles.

In figure 18 a comparison of the flap noise data is shown at about the same peak flap impingement velocity for two sets of data from the cold flow and engine tests. The data include atmospheric attenuation and are given for a standard day condition of 77° F and 70 percent relative humidity and are for a microphone distance of 100 feet. In figure 18(a) the flap normalized radiation patterns are

compared for the two installations. The agreement is considered good over a large portion of the acoustic circle. The engine data between zero and 30° for the lower velocity test (325 feet per second) were influenced by inlet noise that occurred above 4000 Hz. The increase in OASPL in this region (0 to 30°) due to inlet noise was of the order of 1.0 dB. For the higher flap impingement velocity (445 feet per second) this effect was negligible.

Normalized sound pressure level spectra at 70° from the engine (nozzle) inlet are compared in figure 18(b) and (c) for the two sets of nominally similar flap impingement velocities. The spectral data in figure 18(b) and (c) are in general agreement over the entire frequency range.

In figure 19 the normalized OASPL at 70° and at 100 feet is shown as a function of the peak flap impingement velocity for the engine and cold flow tests. Engine data for a nozzle-to-flap distance of 91 inches (fig. 16) are presented. For comparison, a 6th power relation is indicated by the curve. At a given velocity, the normalized OASPL for the engine-wing configuration is slightly higher than that for the cold flow facility.

The projected area concept gives a reasonably close approximation when scaling data from the two different EBF tests using mixer nozzles. In addition, the data from the two facilities show similar trends. That is, OASPL follows a 6th power relation of peak flap impingement velocity, and the directivity patterns and spectral shapes are similar.

CONCLUDING REMARKS

Results from tests of a large scale model of an EBF system employing a mixer nozzle show that for the particular two-flap configuration tested no benefit arises, when compared to a conical nozzle, when the trailing flaps were placed in the 20° position (powered lift takeoff condition). The particular mixer nozzle tested met the original design requirements of reducing the exhaust-jet peak velocity to about 60 percent of the nozzle exhaust velocity at the flap impingement point. However, the mixer nozzle geometry produced a radial displacement of the peak velocity location which was detrimental to the acoustic performance. When the trailing flap was raised to a takeoff setting (20° from wing chord line) it was still subjected to a relatively high velocity as a result of the peak velocity radial displacement. In contrast, with the conical nozzle, much of the high velocity portion of the exhaust plume missed the flap system at this setting.

With the trailing flap in a more deflected setting (60° from wing chord line) the noise levels with the mixer nozzle were lower than when a conical nozzle was used. This reduction in flap noise resulted from the reduction in peak impingement velocity with the mixer nozzle. However, the impingement area of the mixer nozzle exhaust plume was greater than that for the conical nozzle and, consequently, partially offset the benefit of reduced impingement velocity.

A comparison of flap noise results from the cold-flow facility with those from a full-scale engine test showed reasonably good agreement when OASPL was plotted as a function of flap impingement velocity. The OASPL under the wing (70° from engine inlet) varied in both tests as the 6th power of peak flap impingement velocity. Model data were scaled to engine test conditions by adjusting sound pressure levels by the ratio of projected flap impingement areas, and shifting the frequency by the ratio of the nozzle total equivalent diameters. Flap noise spectra for the cold-flow and engine tests also showed good agreement when scaled in this manner.

It is concluded from the data and the analysis presented herein that, in general, the flap noise characteristics of mixer nozzle - EBF systems can be understood on the basis of consideration of both the peak impingement velocity and the impingement area.

SYMBOLS

A_i impingement area, ft^2

A_p projected flap area, ft^2

C_e nozzle discharge coefficient

D_{et} equivalent diameter = $\sqrt{\frac{4 \text{ (Total area)}}{\pi}}$, inches

D_o distance across nozzle lobes, inches

M_j Mach number at nozzle exit

r radial distance from nozzle axis, inches

V free-stream peak jet velocity, ft/sec

V_j peak velocity at nozzle exit, ft/sec

X axial distance from nozzle exit, ft/sec

REFERENCES

1. Dorsch, R. G., Krejsa, E. A., and Olsen, W. A., "Blown Flap Noise Research," AIAA Paper 71-745, Salt Lake City, Utah, 1971.

2. von Glahn, U. H., Groesbeck, D. E., and Huff, R. G., "Peak Axial-Velocity Decay with Single-and Multi-Element Nozzles," AIAA Paper 72-48, San Diego, Calif., 1972.

3. Ciepluch, C. C., North, W. J., Coles, W. D., and Antl, R. J., "Acoustic, Thrust, and Drag Characteristics of Several Full-Scale Noise Suppressors for Turbojet Engines," TN 4261, 1958, NACA.

4. Putnam, T. W., and Lasagna, P. L., "Externally Blown Flap Impingement Noise," AIAA Paper 72-664, Boston, Mass., 1972.

5. Lasagna, P. L., and Putnam, T. W., "Externally Blown Flap Impingement Noise," NASA SP-320, 1972, pp. 427-441.

6. Samanich, N. E., Heidelberg, L. J., and Jones, W. L., "Effect of Nozzle Configuration on Aerodynamic and Acoustic Performance of an Externally Blown Flap System with a Quiet 6:i Bypass Ratio Engine," AIAA Paper 73-1217, Las Vegas, Nev., 1973.

7. Goodykoontz, J. H., Olsen, W. A., and Dorsch, R. G., "Small-Scale Tests of the Mixer Nozzle Concept for Reducing Blown-Flap Noise," TM X-2638, 1972, NASA.

8. Goodykoontz, J. H., Dorsch, R. G., and Groesbeck, D. E., "Noise Tests of a Mixer Nozzle-Externally Blown Flap System," TN D-7236, 1973, NASA.

9. Goodykoontz, J. H., Wagner, J. M., and Sargent, N. B., "Noise Measurements for Various Configurations of a Model of a Mixer Nozzle-Externally Blown Flap System," TM X-2776, 1973, NASA.

10. Dorsch, R. G., Kreim, W. J., and Olsen, W. A., "Externally-Blow-Flap Noise," AIAA Paper 72-129, San Diego, Calif., 1972.

11. Dorsch, R. G., Goodykoontz, J. H., Sargent, N. B., "Effect of Configuration Variations on Externally Blown Flap Noise," AIAA Paper 74-190, Washington, D.C., 1974.

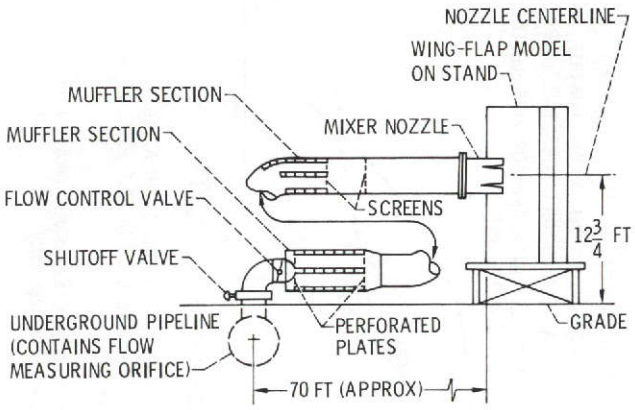

FIGURE 1. - NOZZLE AIR SUPPLY SYSTEM FOR COLD FLOW FACILITY.

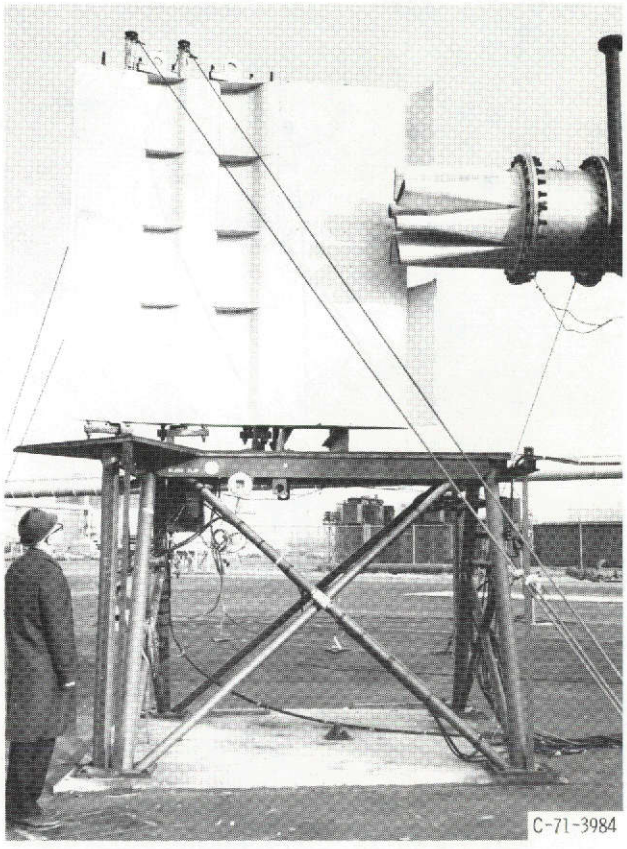

Figure 2. - Test installation.

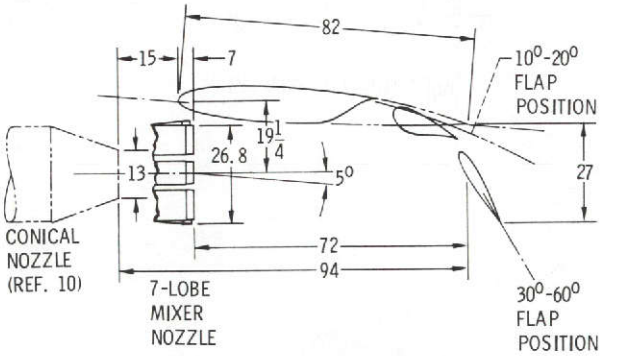

(a) WING-NOZZLE GEOMETRY.

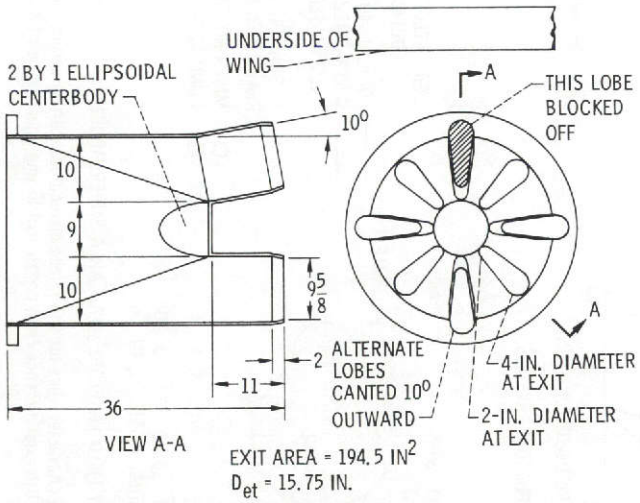

(b) MIXER NOZZLE.

FIGURE 3. - CONFIGURATION AND DIMENSIONS OF THE COLD-FLOW EBF SYSTEM (ALL DIMENSIONS IN IN.)

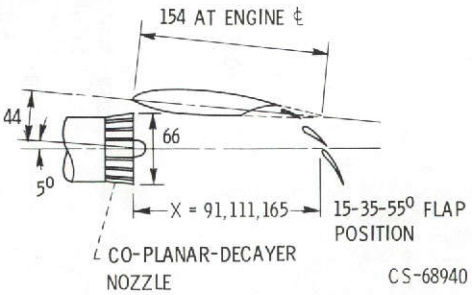

Figure 4. - Full scale engine exhaust nozzle and wing orientation (ref. 6). (All dimensions in inches.)

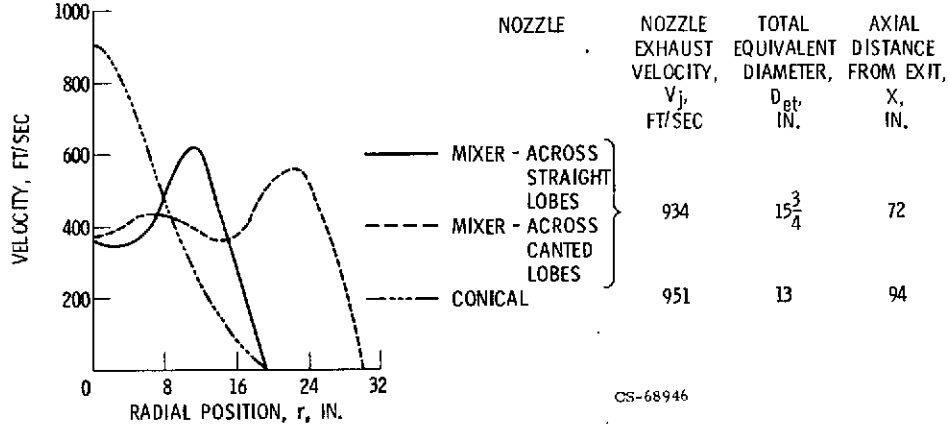

(A) VELOCITY PROFILES.

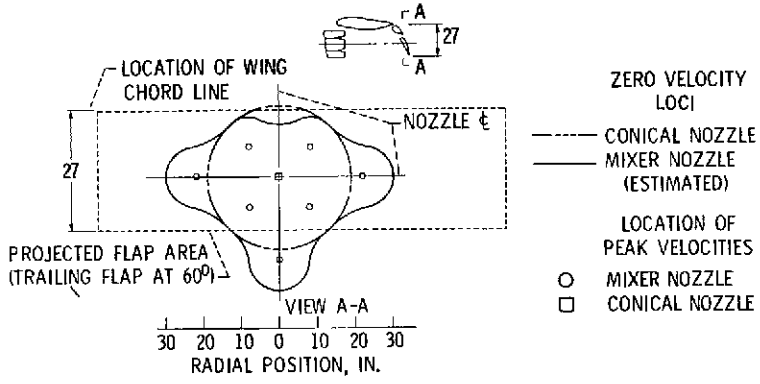

(B) FLOW FIELD ENVELOPE (FLAP AREA SUPERIMPOSED).

Figure 5. - External flow characteristics for the 7-lobe mixer nozzle and a conical nozzle, with wing removed, at the axial distance from nozzle exit to impingement point on 60° trailing flap.

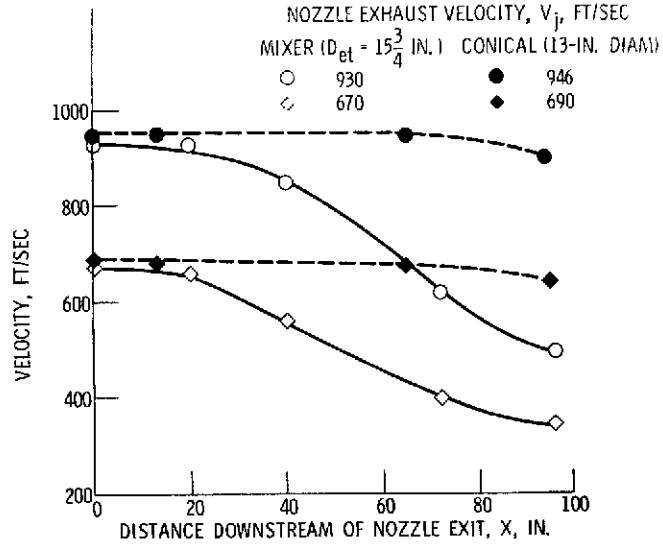

(A) LOCAL PEAK VELOCITIES FOR THE MIXER AND CONICAL NOZZLES.

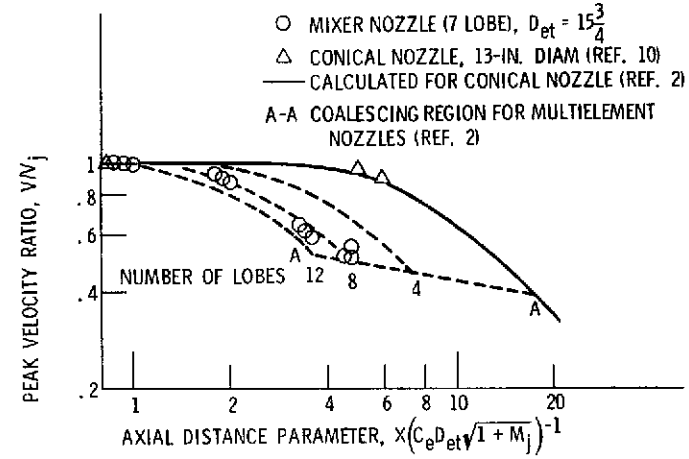

(B) VELOCITY DECAY AS A FUNCTION OF AN AXIAL DISTANCE PARAMETER BASED ON NOZZLE TOTAL EQUIVALENT DIAMETER.

Figure 6. - Comparison of peak axial velocity decay for the 7-lobe mixer nozzle and conical nozzle.

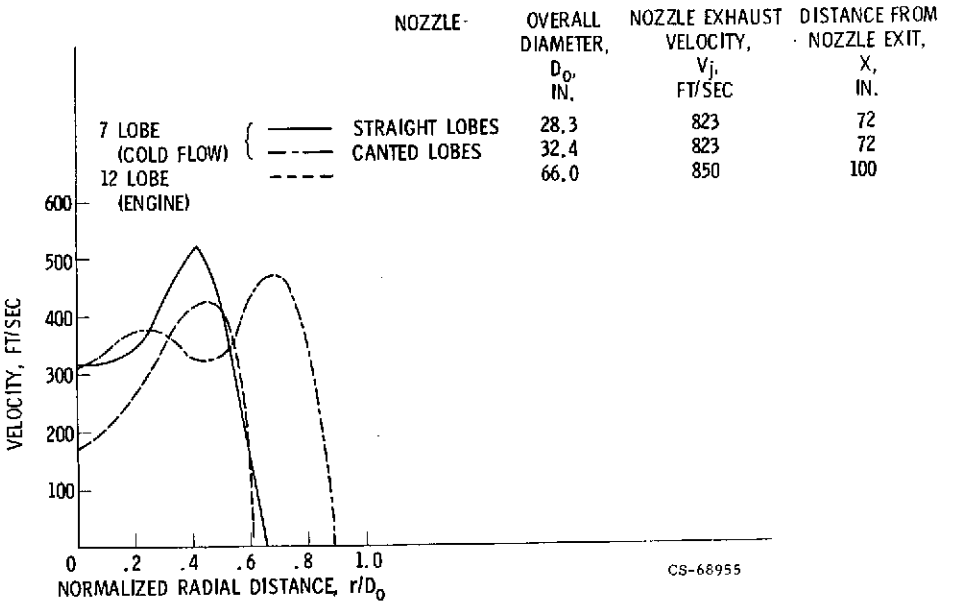

Figure 7. - Velocity profiles across nozzles of cold flow and engine nozzles (wing removed).

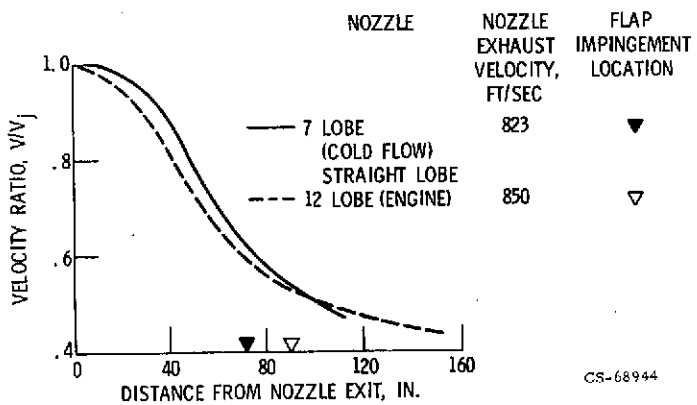

Figure 8. - Peak axial velocity decay for the cold flow and engine nozzles.

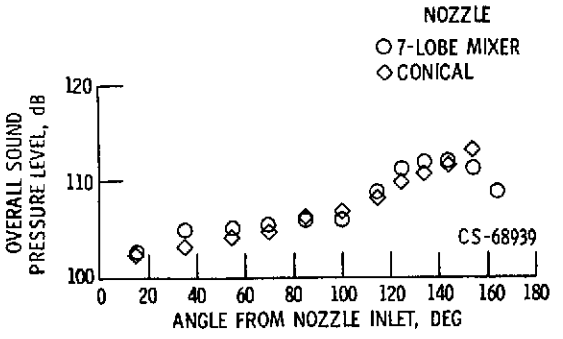

(A) OVERALL SOUND PRESSURE LEVEL DIRECTIVITY.

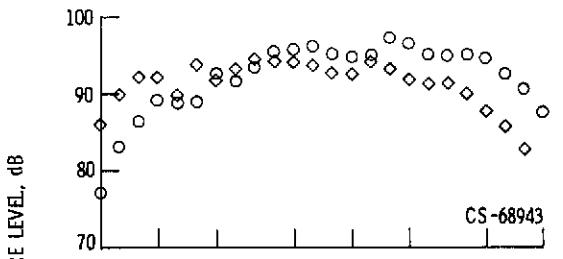

(B) SOUND PRESSURE LEVEL 1/3 OCTAVE SPECTRA AT 85°.

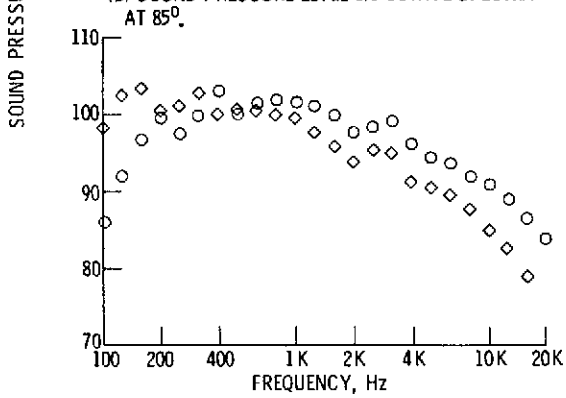

(C) SOUND PRESSURE LEVEL 1/3 OCTAVE SPECTRA AT 145°.

Figure 9. - Comparison of noise data for the 7-lobe mixer nozzle alone and a conical nozzle alone. Nozzle exhaust velocity, 935 ft/sec; microphone distance, 50 feet.

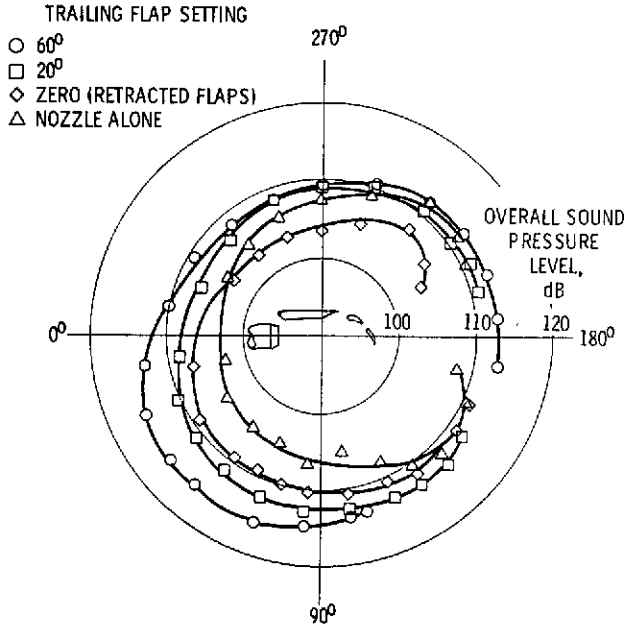

(A) OVERALL SOUND PRESSURE LEVEL DIRECIVITY.

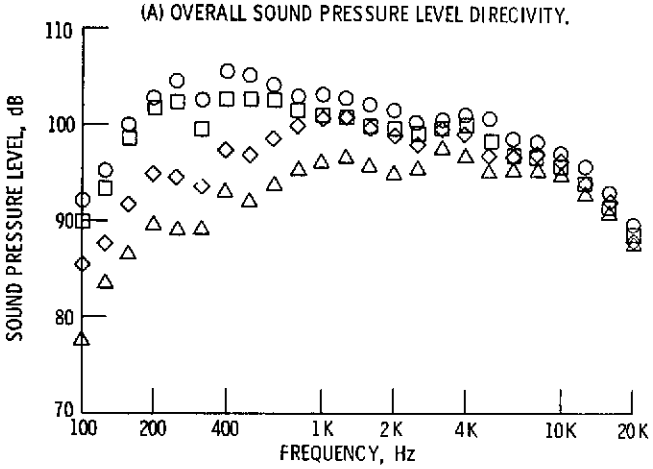

(B) SOUND PRESSURE LEVEL 1/3 OCTAVE SPECTRA AT 85°.

Figure 10. - Noise data for the 7-lobe mixer nozzle and wing with various flap settings. Nozzle exhaust velocity 935 ft/sec; microphone distance, 50 feet.

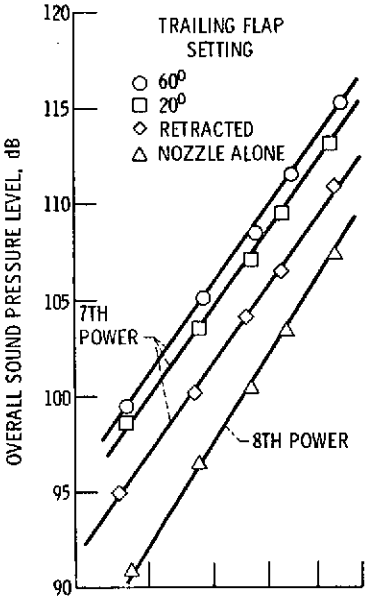

(A) 85° FROM NOZZLE INLET.

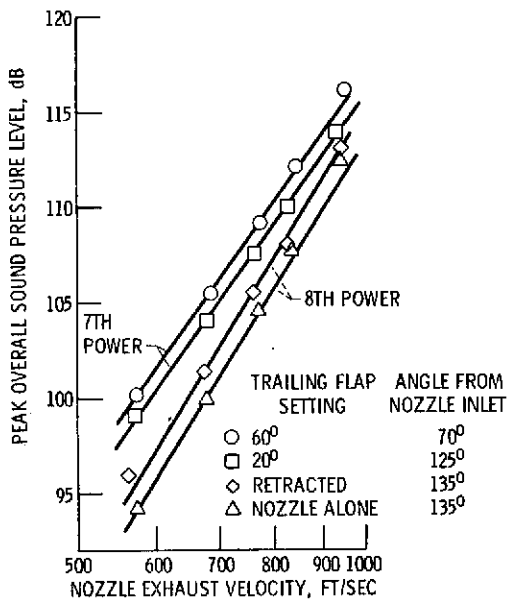

(B) PEAK OVERALL SOUND PRESSURE LEVEL.

Figure 11. - Variation of overall sound pressure level with nozzle exhaust velocity for the 7-lobe mixer nozzle with and without the wing. Microphone distance, 50 feet.

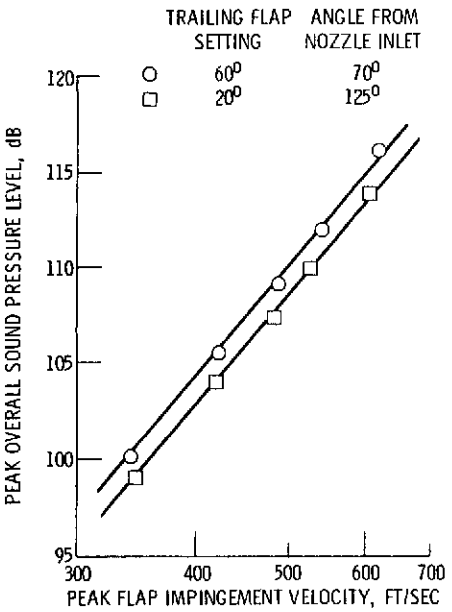

Figure 12. - Peak overall sound pressure level as a function of peak flap impingement velocity for the 7-lobe mixer nozzle with the wing. Microphone distance, 50 feet.

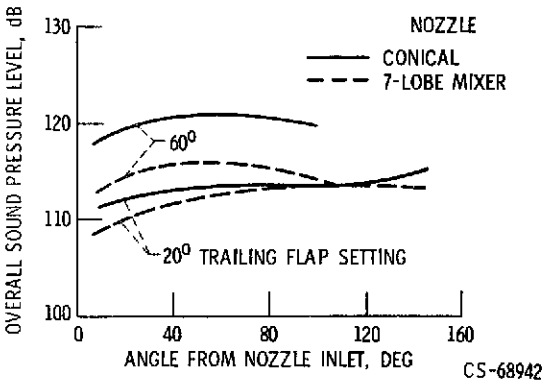

(A) OVERALL SOUND PRESSURE LEVEL DIRECTIVITY.

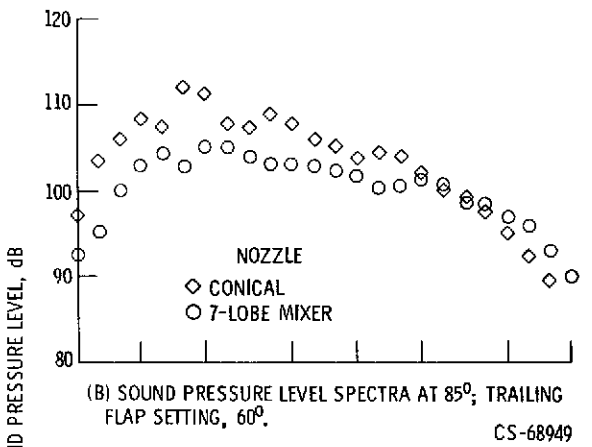

(B) SOUND PRESSURE LEVEL SPECTRA AT 85°; TRAILING FLAP SETTING, 60°.

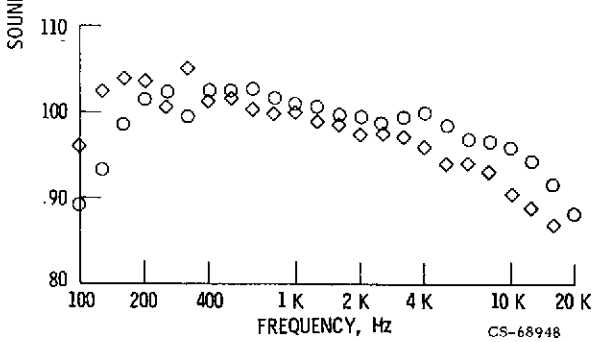

(C) SOUND PRESSURE LEVEL SPECTRA AT 85°; TRAILING FLAP SETTING, 20°.

Figure 13. - Comparison of noise data for the 7-lobe mixer and conical nozzles with the wing with various trailing flap settings. Nozzle exhaust velocity, 943 ft/sec; microphone radius, 50 feet.

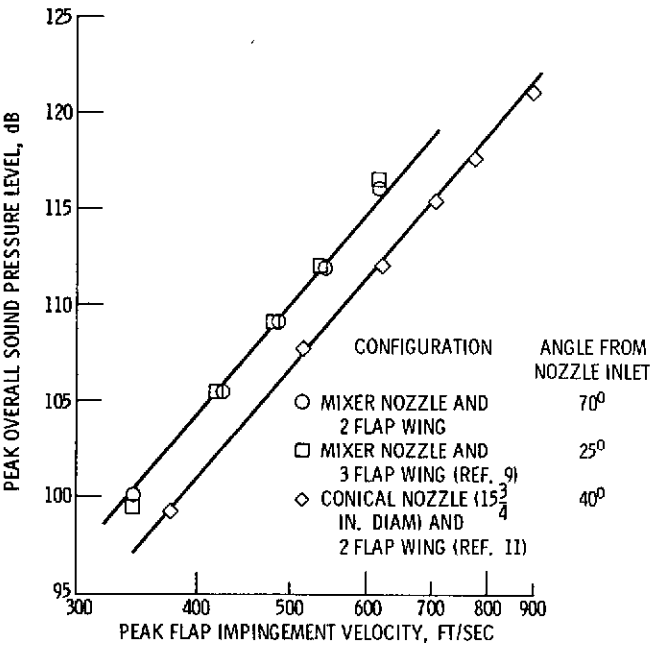

Figure 14. - Peak overall sound pressure level as a function of peak flap impingement velocity for the 7-lobe mixer nozzle with a two- and three-flap wing and the conical nozzle with the two-flap wing. Trailing flap setting, 60°; microphone distance, 50 feet.

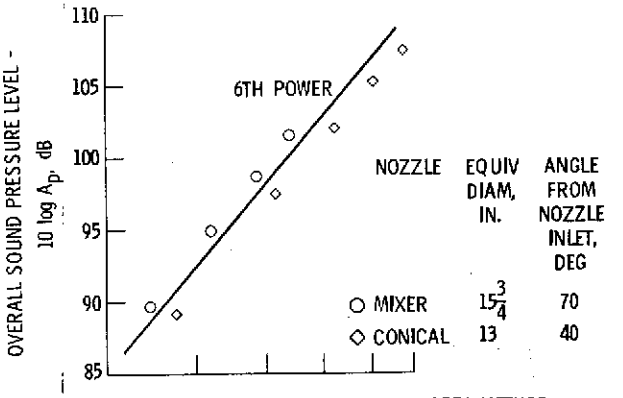

(A) SCALED BY PROJECTED FLAP AREA METHOD.

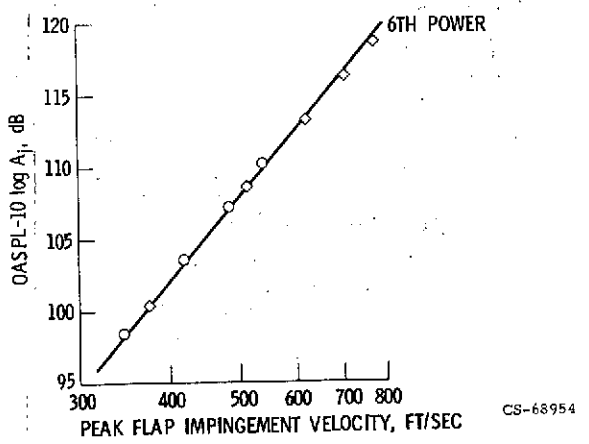

(B) SCALED BY IMPINGEMENT AREAS OCCURING AT 80 PERCENT OF PEAK VELOCITY.

Figure 15. - Normalized peak overall sound pressure as a function of peak flap impingement velocity for the 7-lobe mixer nozzle and conical nozzle. Trailing flap setting, 60^0; microphone distance, 50 feet.

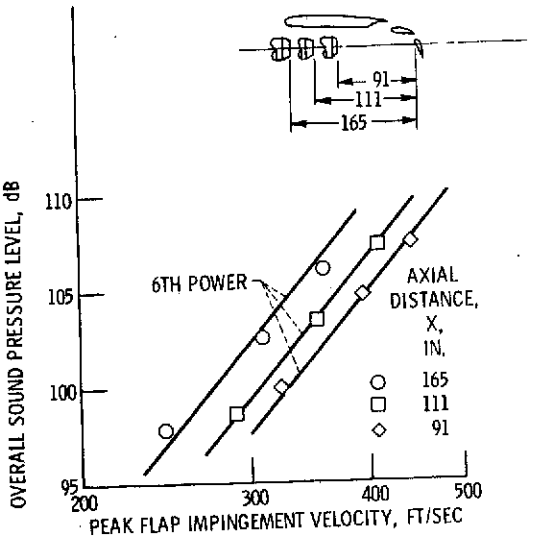

Figure 16. - Overall sound pressure level at 70^0 from engine inlet as a function of peak flap impingement velocity and axial distance from nozzle exit to flap impingement point. Full scale engine data. Trailing flap, 55^0; microphone radius, 100 feet.

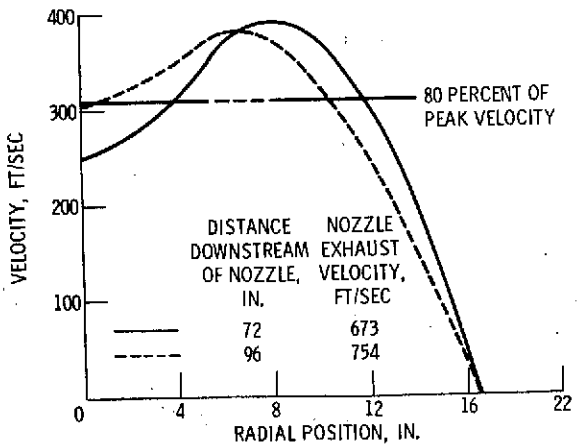

Figure 17. - Comparison of high velocity impingement areas at two distances downstream of nozzle exit. Seven-lobe mixer nozzle.

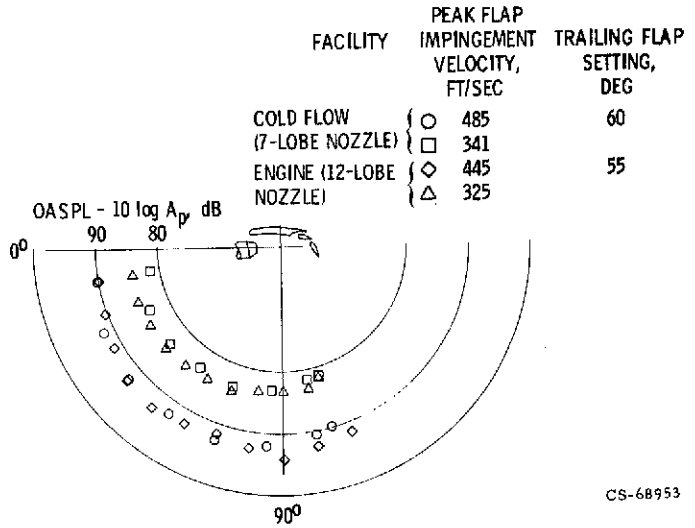

(A) NORMALIZED OVERALL SOUND PRESSURE LEVEL DIRECTIVITY PATTERNS.

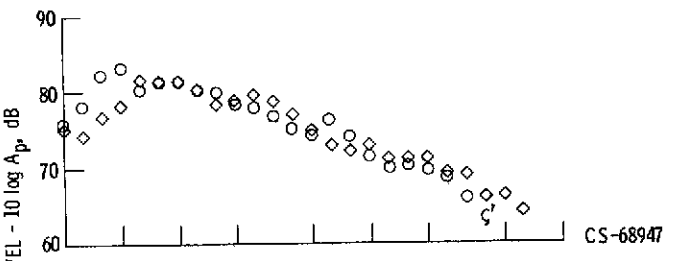

(B) NORMALIZED SOUND PRESSURE LEVEL SPECTRA AT 70^0.

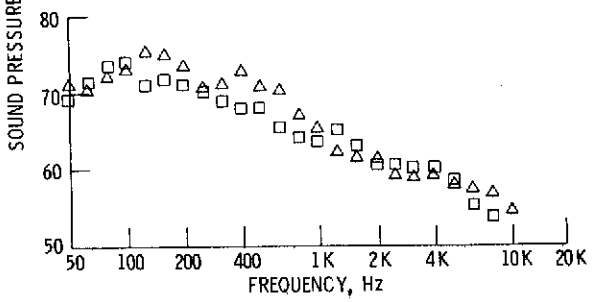

(C) NORMALIZED SOUND PRESSURE LEVEL AT 70^0.

Figure 18. - Comparison of noise data for the cold flow and full scale engine tests. Microphone radius, 100 feet.

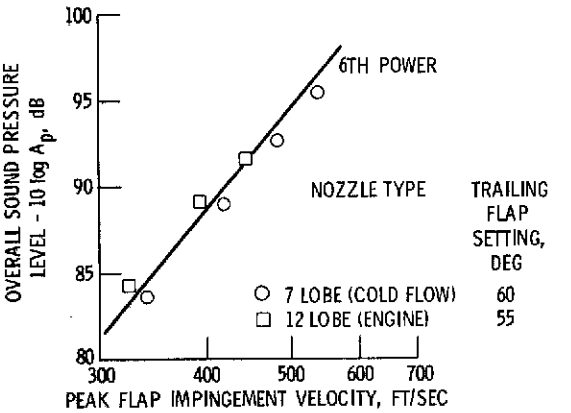

Figure 19. - Normalized overall sound pressure level at 70^0 from nozzle inlet as a function of peak flap impingement velocity for the 7-lobe nozzle cold flow and 12-lobe nozzle engine tests. Microphone distance, 100 feet.